

# Nonequilibrium Solidification in Single Crystal Ni-Base Superalloy<sup>†</sup>

Hu Zhuangqi, Wang Huaming, Zhang Jinghua, Tang Yajun  
Guan Hengrong

**Abstract:** Single crystal superalloys have excellent high temperature mechanical properties. Some interesting results of nonequilibrium solidification in single crystal superalloys have been obtained, including: selection of solid/liquid interface morphology to determine how to control processing parameters of directional solidification; solidification under very high thermal gradient and lateral constraint; first observation of a ( $\gamma + \gamma'$ ) eutectic-free zone and a new TiC morphology.

**Keywords:** nickel-base superalloy; nonequilibrium solidification; single crystal

## 1 Introduction

Superalloy has very excellent high temperature properties, such as elevated temperature stress rupture, creep, fatigue and good oxidation and corrosion resistance. Therefore, it is widely used as the most important and critical parts used at elevated temperature in airplane engines, gas turbines and petrochemical equipments. A lot of service experience and failure analysis showed that the grain boundary is weaker part when it was subjected under stress and at elevated temperature. Microcrack usually creates along transverse grain boundary. Therefore, a directionally solidified superalloy lack of transverse grain boundary has been developed. The direction of solidification is parallel to that of the applied stress, so that the elevated temperature rupture strength and ductility as well as the thermal fatigue resistance are significantly improved. The longitudinal grain boundary becomes a new weaker part in directionally solidified superalloy. It is necessary to eliminate completely all kinds of grain boundaries in order to further enhance the mechanical properties. In this case, a single crystal superalloy

---

<sup>†</sup> 本文原载于《有色金属冶金及材料国际学术会议论文集》，1996，400~409.

\* Institute of Metal Research, Academia Sinica, Shenyang, 110015, China.

produced by directional solidification and crystal selector technology possesses an extraordinary progress than directionally solidified superalloy<sup>[1 2]</sup>.

Processes of directional solidification mainly are high rate solidification process (HRS), liquid metal cooling process (LMC) and zone melting liquid metal cooling (ZMLMC). However after comparison the high rate solidification process is a commonly used main process in the industry, because it is easy to be used in the industry and can not be polluted by metal with low melting point.

Generally the solutioning heat treatment of single crystal superalloy needs very high temperature which makes the size and distribution of phase beneficial to the improvement of creep strength. Main factors that affect creep property of single crystal superalloy blade are crystallization orientation, surface recrystallization, existence of harmful phase, coarse dendritic structure and large ( $\gamma + \gamma'$ ) eutectic. The developed single crystal superalloys mainly are Ni-base alloys. About forty single crystal superalloys have been developed over the world.

Characterizations of alloying are:

(1) elimination of grain boundary strengthening elements, such as C, B, Zr, etc which usually lower the melting temperature.

(2) addition of large amount of W, Mo, Ta, Nb and Hf elements to the single crystal alloy, generally having a total amount of about 15wt%.

(3) addition of enough Al (5~6wt%) and appropriate Ti (0~4wt%) to ensure to have a sufficient amount of  $\gamma'$  phase.

(4) Re addition (1~3wt%) in new single crystal superalloys to improve mechanical properties (for example PWA1484, CMSX-4G etc).

(5) addition of more Cr in single crystal superalloys used in marine and industrial gas turbine engine blades for having a better hot corrosion resistance (for example RR2060, DD8 etc). There are three kinds of structures of single crystal superalloys. One is dendritic structure, the second is cellular and the third is plane front structure. The segregation is serious in dendritic structure and the properties are the worst. There is no segregation when it is plane front solidification which has best properties. It is important to properly control the thermal gradient (G) and solidification rate (R). According to solidification principle, it is necessary to have a high G and low R.

Recently tremendous researches on single crystal superalloys are taken in the world. It includes the following aspects, alloy design, solidification processing, principles of alloying, orientation effect, decreasing density, oxidation and hot

corrosion, resistance and coating protection, hot isostatic processing, etc. In this paper some research results on nonequilibrium solidification of single crystal superalloy are introduced.

## 2 Experimental Procedures

Single crystal specimens were produced in a home-made high rate directional solidification equipment. The thermal gradient is about 100K/cm. The DD8 alloy composition is (wt%):

Cr 16.0 Co 8.5 W 6 Al 3.9 Ti 3.8 Ta 1 Ni bal

Solidification experiment under lateral constraint was done in another high rate directional solidification vacuum furnace. The thermal gradient ahead of the solidifying interface is about 70K/cm. High thermal gradient experiment was performed in a zone melting liquid metal cooling equipment in Northwestern Polytechnical University. The thermal gradient can reach 1200K/cm. The laserglazing of the single crystal superalloy was treated on a 2kW CO<sub>2</sub> continuous wave laser. The laser beam diameter is about 1mm and the power density is approximately  $1.4 \times 10^5 \text{ W/cm}^2$ .

Using Neophot microscope, Cambridge 360 scanning electron microscope (SEM), Camebax-Micro electron probe microanalyser, EM420 transmission electron microscope, Latex II image analyzer to determine the composition and observe the microstructure.

## 3 Results and Discussions

### 3.1 Selection of Solid/Liquid Interface Morphology

Fig.1 shows solid/liquid interface morphology at different cooling conditions. As the solidification rate increases, the planar interface (Fig.1(a)) destabilizes and transforms to cellular (Fig.1(c)), cellular-dendritic (Fig.1(d)), coarse dendritic (Fig.1(e)) and finally to fine dendritic (Fig.1(f)) interfaces, which is consistent with the constitutional supercooling theory.

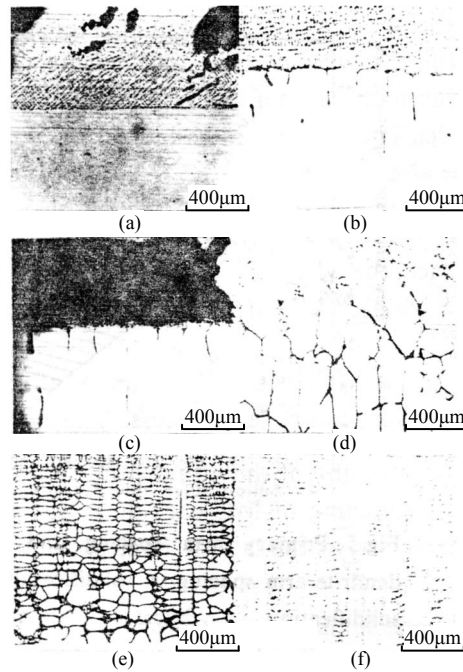


Fig.1 Solidification interface morphologies

- (a) planar solidified at  $1.42\mu\text{m/s}$ ; (b) pertubated planar solidified at  $2.08\mu\text{m/s}$ ;
- (c) cellular solidified at  $2.17\mu\text{m/s}$ ; (d) cellular-dendritic solidified at  $2.94\mu\text{m/s}$ ;
- (e) coarse dendritic solidified at  $12.6\mu\text{m/s}$ ; (f) fine dendritic solidified at  $110.2\mu\text{m/s}$

Fig.2 shows the variations of dendrite arm spacings as well as cellular or cellular-dendrite spacings with solidification rate. Both the primary and secondary dendrite arm spacings decrease considerably with the increasing solidification rate. Fig.3 denotes the effect of solidification rate on the dendritic or cellular segregation ratios, i.e. the maximum to minimum composition in a dendrite or a cell. It is clearly shown that the segregation ratios increase remarkably as the interface change from cellular to dendritic. The segregation ratios of the dendritic solidified structures decrease markedly as the solidification rate continues to rise, as the coarse dendritic transforms into fine one.

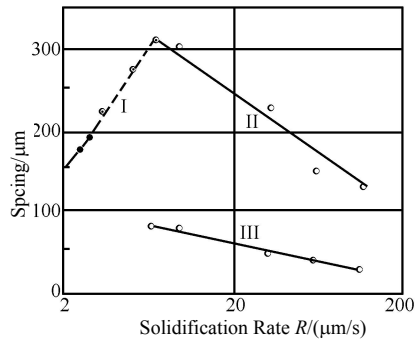


Fig.2 Primary arm spacing and secondary dendrite arm spacing as a function of solidification rate and solidification interface shape under conventional low temperature gradient solidification conditions

●cellular; ○cellular-dendritic; ○dendritic  
 I--cell or cellular dendrite spacing; II--primary dendrite arm spacing; III--secondary dendrite arm spacing

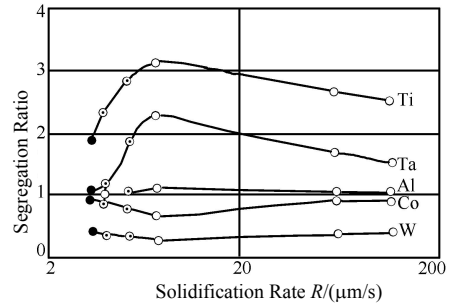


Fig.3 Variation of segregation ratio of solute with solidification rate and interface morphologies

●cellular; ○cellular-dendritic; ○dendritic

Fig.4 illustrates the curve of solute segregation in the interdendritic  $\gamma/\gamma'$  eutectic region under different solidifying rates. In the fine Structure differences are rather small between an extremely fine  $\gamma/\gamma'$  eutectic and its surrounding matrix, as shown in Fig.4(a) which are easy to be homogenized. On the contrary, P, Ti, Ta in the coarse well-developed  $\gamma/\gamma'$  eutectic are extremely enriched and Cr, W, Co are highly depleted. It is very difficult or impossible to eliminate the heavily segregated regions by homogenization treatment.

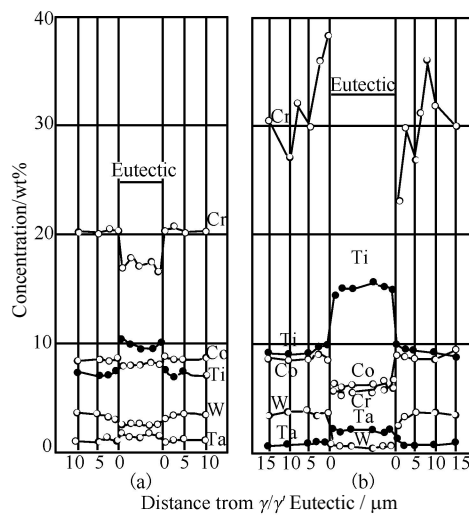


Fig.4 Solute distribution in interdendritic  $\gamma/\gamma'$  eutectic region

(a) fine dendrite structure solidified at 110.2  $\mu\text{m/s}$ ; (b) coarse dendrite structure solidified at 6.67  $\mu\text{m/s}$

Generally it is better to get solidification rate as low as possible, but from our experimental condition the solidification rate is better to be controlled as fast as possible in order to turn the coarse dendrite into fine dendrite and get low segregation levels. Coarse dendritic structure must be avoided<sup>[3,4]</sup>.

### 3.2 Solidification of Single Crystal Superalloy under Very High Thermal Gradient

According to the constitutional undercooling theory, it is best to have a very high temperature gradient to keep plane front solidification. But the thermal gradient of high rate solidification can only reach the level of 100K/cm, a new zone melting liquid metal cooling (ZMLMC) process was used to raise the thermal gradient ten times higher than HRS. The effect of high thermal gradient on the solidification process was studied<sup>[5]</sup>.

#### 3.2.1 Effect on the interface morphology

Fig.5 shows the effect of solidification rate on the interface morphology. By using ZMLMC, the morphology of solid/liquid interface transforms from plane front to cellular at 100 $\mu\text{m/s}$ , but at 3 $\mu\text{m/s}$  when HRS is used.

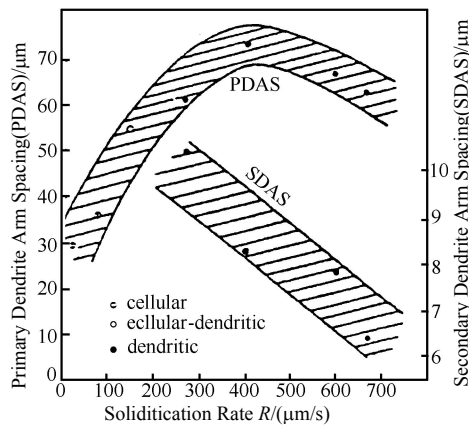


Fig.5 Primary arm spacing and secondary dendrite arm spacing vs solidification rate and solidification interface morphology under ultra-high temperature gradient solidification conditions

#### 3.2.2 Effect on the cellular spacing

Cellular spacing in HRS process is about 200 $\mu\text{m}$  and it is just below 40 $\mu\text{m}$  in ZMLMC process that makes the cellular structure much finer.

#### 3.2.3 Effect on the dendritic arm spacing

Primary and secondary dendritic arm spacing is 300 $\mu\text{m}$  and 60 $\mu\text{m}$  respectively

when HRS process is used. By using ZMLMC it decreases to about 70 $\mu\text{m}$  and 30 $\mu\text{m}$ . The primary dendritic arm spacing is increased with the rise of the solidification rate. When the solidification rate is above 400 $\mu\text{m}/\text{s}$ , the primary dendritic arm spacing becomes finer. This is because the solidification process of dendrites is restricted by space-time condition of rapid solidification.

### 3.2.4 Effect on the nonequilibrium $\gamma/\gamma'$ eutectic

The  $\gamma/\gamma'$  eutectic appears when the cellular transforms to dendritic, but the  $\gamma/\gamma'$  eutectic size in ZMLMC is much smaller than that in HRS. The former is about 4 $\mu\text{m}$  and the latter is about 10 $\mu\text{m}$ , The  $\gamma/\gamma'$  eutectic size becomes smaller when the cooling rate increases in ZMLMC, and  $\gamma'$  phase in eutectic becomes smaller correspondingly. The size is about 0.3 $\mu\text{m}$ .

### 3.2.5 Effect on microporosity

As shown in Fig.6 the microporosity in ZMLMC is significantly smaller than in HRS. The former is about 0.05~0.2 vol%, while the latter is 0.4~0.9vol%. In addition the microporosity increases with the solidification rate in ZMLMC, but when the solidification rate is at 400 $\mu\text{m} \cdot \text{s}^{-1}$ , that is to say the primary dendritic arm spacing becomes finer, the microporosity also becomes smaller.

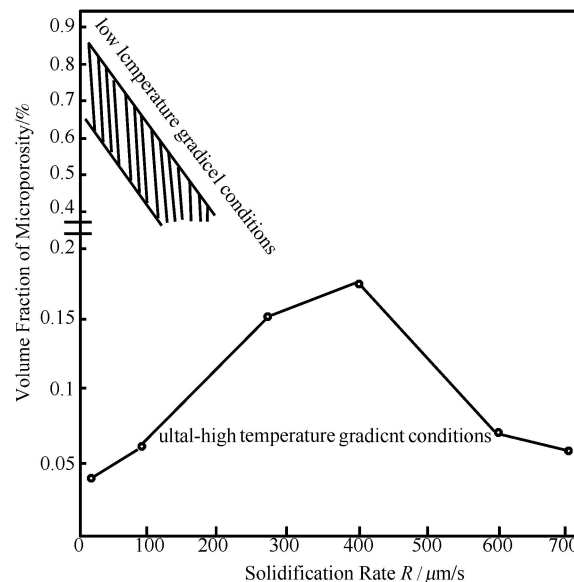


Fig.6 Volume fraction of microporosity as a function of solidification rate and temperature gradient conditions

## 3.3 Solidification of Single Crystal Superalloy under Lateral Constraint

Fig.7 shows the cross-section of specimen suddenly decreases when it is

under lateral constraint<sup>[6]</sup>. The transformation of the solidification structure of single crystal superalloy is shown in Fig.8. The lateral constraint condition has a great influence on the solidification morphology of single crystal superalloy. The solidification structure transforms fastly from coarse dendrite to very fine cellular when the cross-section of specimen suddenly decreases. As the solidification goes on, the cellular spacing gets larger and then to be stable. At last, when the cross-section of specimen suddenly increases, the morphology of single crystal superalloy transforms from cellular to dendritic. The other new and interesting result was found as shown in Fig. 8(b). The mechanism of transformation from cellular to dendritic structure is not the perturbation from the lateral cell wall. Instead of it, it is first unstable at the cell tips where are split into two pans. It can be explained due to the restriction of space-time condition of local cooling condition. In the other hand the as-solidified structure morphology of single crystal transforms from dendritic to cellular, it passes a transition zone when the cross-section of specimen decreases suddenly as shown in Fig.8. The dendrites in this zone are very fine, and no  $\gamma/\gamma'$  eutectic-free zone (Fig.9). It can also evidence that the solute contents of distribution ratio below one in eutectic-free zone greatly decreases. Afterwards in cellular solidification region the solute concentrations rapidly increase steadily. At last when the cross-section of specimen increases suddenly and it resolidifies into dendritic region. The solute concentration rapidly increases again (Fig.10).

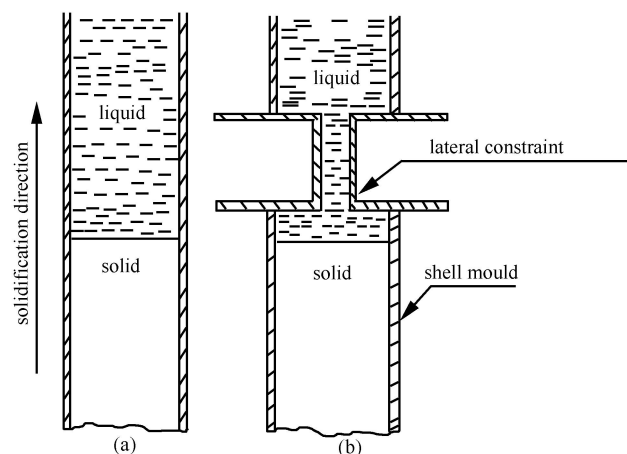


Fig.7 Illustration of the experimental arrangement  
(a) without lateral constraint; (b) with lateral constraint

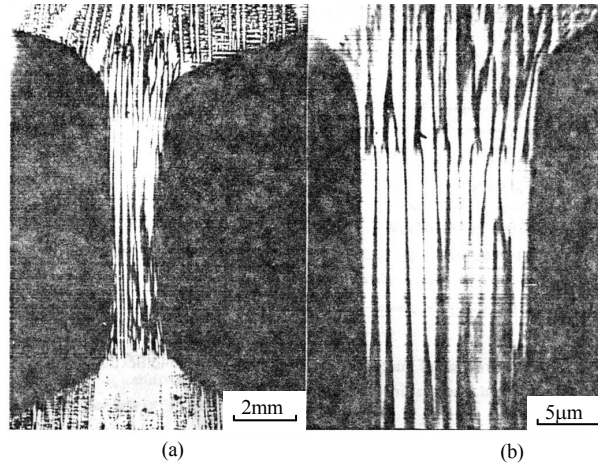


Fig.8 Change of solidification structure caused by a reduced section (from 16mm to 4mm in diameter) of a single crystal superalloy specimen. The arrow indicates the solidification direction  
 (a) low magnification; (b) high magnification

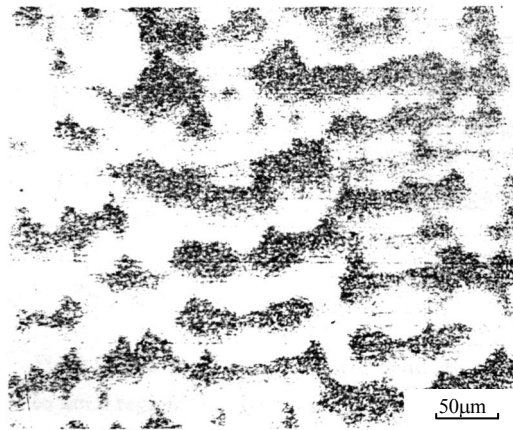


Fig.9 Microstructure of single crystal superalloy under lateral constraint, showing eutectic-free region

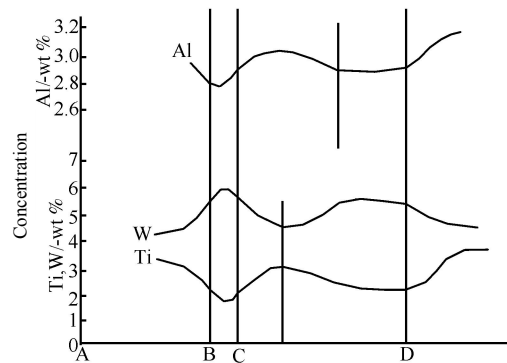


Fig.10 Solute profiles along the longitudinal direction of the reduced section of sample under lateral constraint

A-B: large cross-section; B-C: transition to reduced cross-section; C-D: small cross-section

When the cross-section of single crystal specimen suddenly decreases in directional solidification, it must lead to the increase of the thermal gradient ( $G$ ) and solidification rate ( $R$ ) greatly in this local region. As shown in Fig.11, it is just because the cooling rate ( $G \cdot R$ ) is very high in this time, that refines the solidified structure and reduces the solute segregation, which results in the formation of eutectic-free zone.

It can not use constant withdrawal rate in production when the cross-section of single crystal casting changes suddenly. The withdrawal rate and other cooling condition should be adjusted on time in the whole directional solidification process in order to obtain uniform structure and composition of single crystal casting.

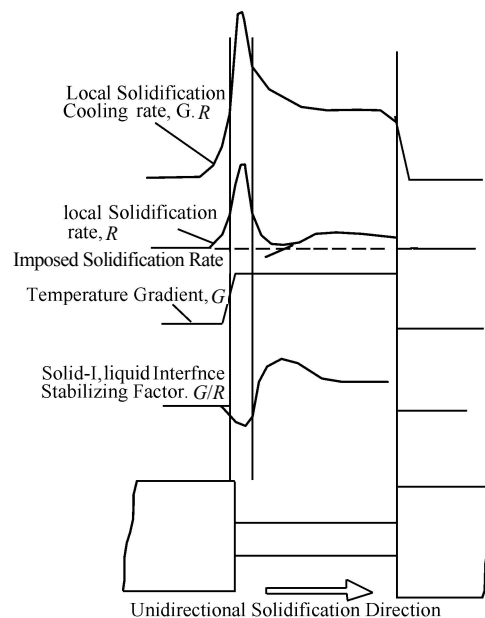


Fig.11 Illustrations of the dynamical changes in local solidification cooling parameters due to the presence of a lateral constraint

### 3.4 Carbide Morphology in Single Crystal Superalloy

It has a great effect of primary carbide on the mechanical properties, even on casting properties, of Ni-base superalloy. There are two types of TiC in the commercial Ni-base superalloys, one is blocky morphology and another is Chinese-script morphology. The third type of TiC morphology was found in rapidly solidified single crystal superalloy. Fig.12 shows the TiC morphology at the cooling rate  $1.4 \times 10^5 \text{ K/s}$ <sup>[7]</sup>, Morphologies of TiC are all in radiated forms. They all

grow from nucleation and develop from flower-like to well-developed highly and radially branching colonies. These metastable structures, far away from equilibrium condition, have the characterization of fractal. According to the analysis, the calculated lattice constants of the TiC range from 0.43 to 0.46nm, because a certain amount of Ta, Co, Cr, etc. are also present in this carbide besides Ti due to rapid solidification. From the figure, the facet and the growing step can be also observed.

During rapid solidification the eutectic reaction  $L \rightarrow (\gamma + MC)$  takes place in the interdendritic solute-enriched liquid, and hence the MC/ $\gamma$  eutectic growth process is associated with the morphology of MC carbide, and MC carbide is the leading nucleation phase for the eutectic reaction.

It is natural that the growth morphology of MC carbide is strongly affected by cooling rate since the eutectic growth is diffusion controlled process. The higher the solidification cooling rate, the deeper the undercooling of the liquid, the lower the atom diffusion. As a result the magnitude of branching of MC carbide in the eutectic cooling increases with increasing cooling rate. It shows the lateral ledge growth mechanism of this kind of TiC morphology<sup>[8]</sup>.



Fig.12 TEM bright field images of the interdentritic MC carbide in. well-developed, highly radially branching colony produced at cooling rate of  $1.4 \times 10^5$  °C/s (carbon Extraction replica)

## 4 Conclusions

(1) Both solidified microstructure and solute segregation behaviors of the single crystal Ni-base superalloy has been remarkably influenced by the

solidification interface morphology. The solute segregation is most serious in the case of the presence of coarse dendrite.

(2) Increase the thermal gradient can refine the cellular or dendritic structure as well as the size of  $\gamma/\gamma'$  eutectic, and reduce the microporosity.

(3) Under lateral constraint solidification, a eutectic-free zone was found and a new cell tip splitting mechanism during the transformation from cell to dendrite was also observed.

(4) A third kind morphology of TiC was found in rapidly solidified Ni-base superalloy. It was flower-like. The higher the cooling rate, the more well-developed the branching. This belongs to a mechanism of lateral ledge growth.

## References

- [1] Hu Z Q. Avia. Prod. Eng., 1987, 2: 12
- [2] Hu Z Q. Avia. Prod. Eng., 1989, 4: 19
- [3] Wang H M, Tang Y J. Acta Metall. Sin., 1991, 27: A92
- [4] Wang H M, Tang Y J et al. Chin. J. Met. Sci. Techno. I, 1991, 7: 270
- [5] Wang H M, Hu Z Q, Murata Y, Morinaga M J. Mater. Sci. & Technol., 1993, 9: 25
- [6] Hu Z Q, Wang H M et al. Ist Pacific Rim International Conf. on Advanced Materials and Processing, 1992. 84
- [7] Yu X H, Zhang J H, Hu Z Q. Mater. Trans. JIM, 1993, 4: 669
- [8] Wang H M, Hu Z Q et al. Mater. Sci. Eng., 1992, A156: 109